

24. Knoppien, P., *Drosoph. Inf. Serv.*, 1985, **61**, 101.
25. Markow, T. A., *Behav. Genet.*, 1980, **10**, 552–556.
26. Robertson, H. M., *Anim. Behav.*, 1982, **30**, 1105–1117.
27. Som, A. and Singh, B. N., *Drosoph. Info. Serv.*, 1998, **81**, 202–203.
28. Bryant, E. H., Kence, A. and Kimball, K. T., *Genetics*, 1980, **96**, 975–993.
29. Partridge, L. and Gardner, A., *Am. Nat.*, 1983, **122**, 422–427.
30. Cakir, S. and Kence, A., *Turk. J. Biol.*, 1999, **23**, 433–443.
31. Spiess, E. B., in *Essays in Evolution and Genetics in Honor of Theodosius Dobzhansky* (eds Hecht, M. K. and Steere, W. C.), North Holland, Amsterdam, 1970, pp. 315–379.
32. Parsons, P. A., *Behavioural and Ecological Genetics. A Study in Drosophila*, Clarendon Press, Oxford, 1973.
33. Knoppien, P., Pot, W. and Van Delden, W., *Genetica*, 1980, **51**, 197–202.
34. Ehrman, L., *Behav. Genet.*, 1970, **1**, 111–118.

35. Ehrman, L., *Behav. Genet.*, 1972, **2**, 79–84.
36. Ehrman, L. and Spiess, E. B., *Am. Nat.*, 1969, **103**, 675–680.
37. Averhoff, W. W. and Richardson, R. H., *Behav. Genet.*, 1974, **4**, 207–225.
38. Averhoff, W. W. and Richardson, R. H., *Proc. Natl. Acad. Sci. USA*, 1976, **73**, 591–593.
39. Van den Berg, M. J., Thomas, G., Hendriks, H. and Van Delden, W., *Behav. Genet.*, 1984, **14**, 45–61.

ACKNOWLEDGEMENTS. Financial assistance in the form of research scholarship from Banaras Hindu University to A.S. is gratefully acknowledged.

Received 15 February 2001; revised accepted 24 May 2001

Plio-Pleistocene pedogenic changes in the Siwalik palaeosols: A rock magnetic approach

S. J. Sangode^{†,*}, J. Bloemendal[#], R. Kumar[†] and S. K. Ghosh[†]

[†]Wadia Institute of Himalayan Geology, P.B. 74, Dehradun 248 001, India

[#]Department of Geography, University of Liverpool, Liverpool, L69 7ZT, UK

Thirty-one pedogenic horizons of the Upper Siwalik (Plio-Pleistocene) sequence near Haripur, Himachal Pradesh (HP) in NW Himalaya are studied using rock magnetic properties to investigate their climatic and stratigraphic significance. The palaeosols are characterized by low initial susceptibility (χ_{ir} -mean = 9×10^{-8} m³/kg), high coercivity of remanence (B_{0Cr} -mean = 447 mT), and low frequency-dependent susceptibility (X_{fd} -max = 6%) as a result of predominance of the canted-antiferromagnetic minerals of SD-PSD range. Stepwise acquisition of isothermal remanent magnetization (IRM) to a forward field of 7000 mT and backfield of 1000 mT indicates the presence of high coercivity minerals (goethite and hematite). Rock magnetic properties of pedogenic levels are inferred with reference to parental horizon of each palaeosol profile. Based on selective saturation levels of induced magnetic field, inorganic and organic carbon content and Rb/Sr ratios, new parameters are attempted to infer the relative variation in pedogenic changes of oxidation, hydroxylation and humification. These parameters record dynamic changes in the soil development processes of the Indo-Gangetic foreland basin, suitable for high-resolution stratigraphic correlations and reconstruction of climate change during the Plio-Pleistocene time.

THE Siwalik Group of the Indo-Gangetic Foreland Basin (IGFB) in Himalaya preserves a long record (~18 to

0.5 Ma) of alluvial fan sedimentation, giving rise to rapid lateral lithofacies variations. This resulted in a problem of time-stratigraphic correlation of the exposed sequences throughout the basin. Scanty occurrence of datable fauna restricted an ideal biostratigraphic approach. Whereas magnetostratigraphy has helped only to a limited extent in solving the stratigraphic problems¹, due to less abundance of suitable rock types that could ideally preserve the records of depositional remanence. The sediments of Siwalik province, although deposited in high-energy conditions, have developed thick and multi-storied soil profiles (or palaeosols) that are untapped yet, to investigate their stratigraphic and climatic relevance.

Rock magnetism presents a rapid, economic, non-destructive and quantitative technique that has recently been applied successfully for climatic and stratigraphic studies worldwide^{2,3}. We report here an independent rock magnetic approach on pedogenic horizons from a well-documented section of Upper Siwalik sub-Group (Plio-Pleistocene) in the IGFB of NW Himalaya (Figure 1), to investigate its climatic and stratigraphic applications.

The Siwalik Group represents the most continuous and near complete record of mammalian faunal evolution in South Asia and is well-known for its hominoid primate fossils^{4,5}. Biostratigraphic records indicate a remarkably high bio-diversity during the Siwalik era⁵ and the Plio-Pleistocene transition records a major faunal change related to climate⁶. Thus it is quite relevant to study the soil supporting such healthy co-existence of eco-system and its relation to climate change.

Johnson⁴ described the Siwalik palaeosols as low-grade oxisols to represent alternate wet and dry seasons, proposing its vegetative similarity to the alluvial soils of Ghana, Sudan and Brazil. Using magnetostratigraphic ages, Behrensmeyer *et al.*⁷ derived 13,000–23,000 years as the maximum time for soil formation during Siwaliks. The characteristic ‘ferruginous-carbonate’ association of these palaeosols is described

*For correspondence. (e-mail: sangode@rediffmail.com)

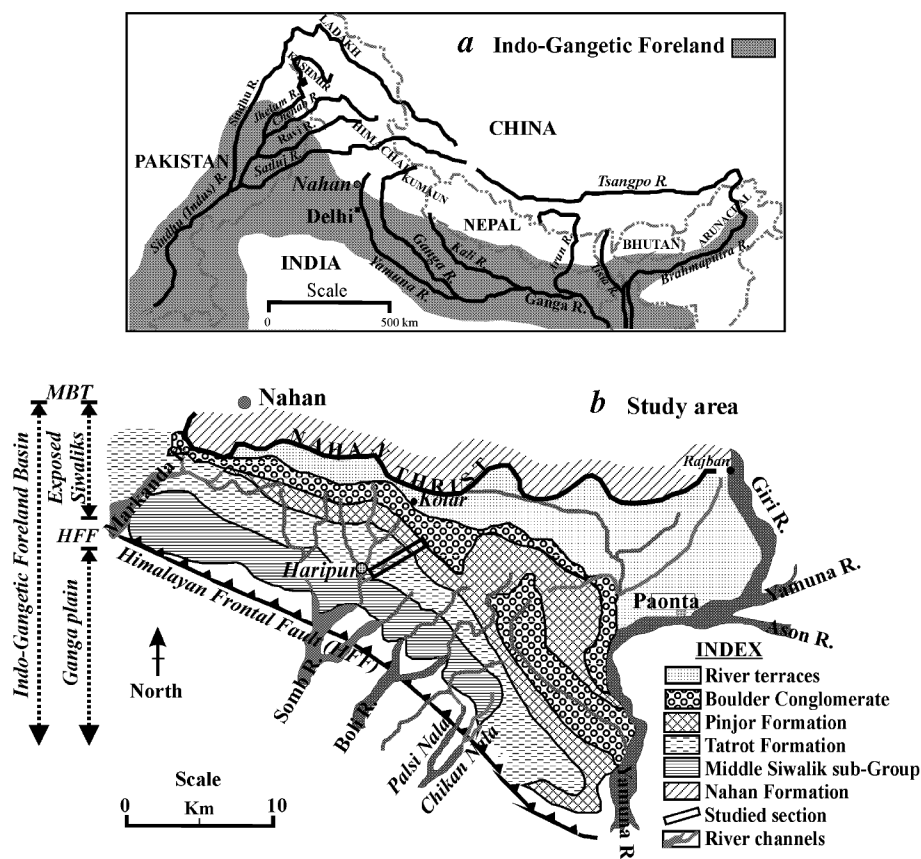


Figure 1. *a*, Geographic extent of Indo-Gangetic Foreland Basin (shaded) with major rivers flowing through. *b*, Geological map of the study area after Srivastava, *et al.*⁹ showing the studied section near Haripur, Nahan Dist. (HP). MBT, Main Boundary Thrust; HFF, Himalayan Frontal Fault.

as a unique and complex phenomenon, representing dry-season oxidative phase followed by wet-season carbonate dissolution phase⁸.

A geological map and biostratigraphic zonation for the study area is given by Srivastava *et al.*⁹ and Nanda *et al.*¹⁰. Detailed sedimentologic and palynostratigraphic aspects for the given section are described elsewhere^{11–13}. Sangode *et al.*¹⁴ reconstructed the chronology for the studied section using magnetostratigraphy. A volcanic ash occurrence at Gauss/Matuyama boundary (2.58 Ma) similar to other well-dated reports in India and Pakistan^{15–17}, confirms the magnetic polarity dates of Sangode *et al.*¹⁴. These studies brought out a good correlation amongst biostratigraphic¹⁰, palynologic¹³ and lithofacies¹¹ formation boundaries for the studied section (Figure 2).

Six palaeosol profiles (comprising 31 pedogenic horizons) were selected for the present investigation considering: (a) the four palaeo-vegetation stages inferred from distribution of pollen/spore taxa¹³; (b) floodplains magnetic susceptibility¹²; (c) sedimentologic events¹¹, and (d) a justifiable distribution with respect to Plio-Pleistocene or Tatrot/Pinjor boundary (marked by volcanic tuff occurrence). Individual palaeosol profiles are

developed on varied parental materials (sandstones/mudstones of different compositions) and are truncated at several places due to encroaching channel activity. In order to enhance the regional scale applicability, we selected only the second story of each composite/multi-storied palaeosol profiles, where parental (C-) horizon of one profile directly overlies the A- or B-horizon of an earlier soil. The youngest profile (HK1) is limited to Mid-Pleistocene, since the later part is dominated by conglomerate facies. Samples were collected by digging at least two feet in a cleaned profile starting from C-horizon upwards to every variegated horizon, subsequently denoted as B1, B2, B3, etc. following the methods suggested by Retallack¹⁸.

Samples from each horizon were prepared in standard non-magnetic pots at the Environmental Magnetic Laboratory (EML), University of Liverpool, UK. Initial susceptibility was computed averaging the value of six specimens each horizon on Bartington's MS-2 sensor for low and high frequency (0.465 and 4.65 kHz) applied fields. Isothermal Remanent Magnetization (IRM) was imparted at intervals of 20/50/100/200 mT up to 4000 mT and back-field to 1000 mT on Molspin and Trilec impulse magnetizers and the remanence was

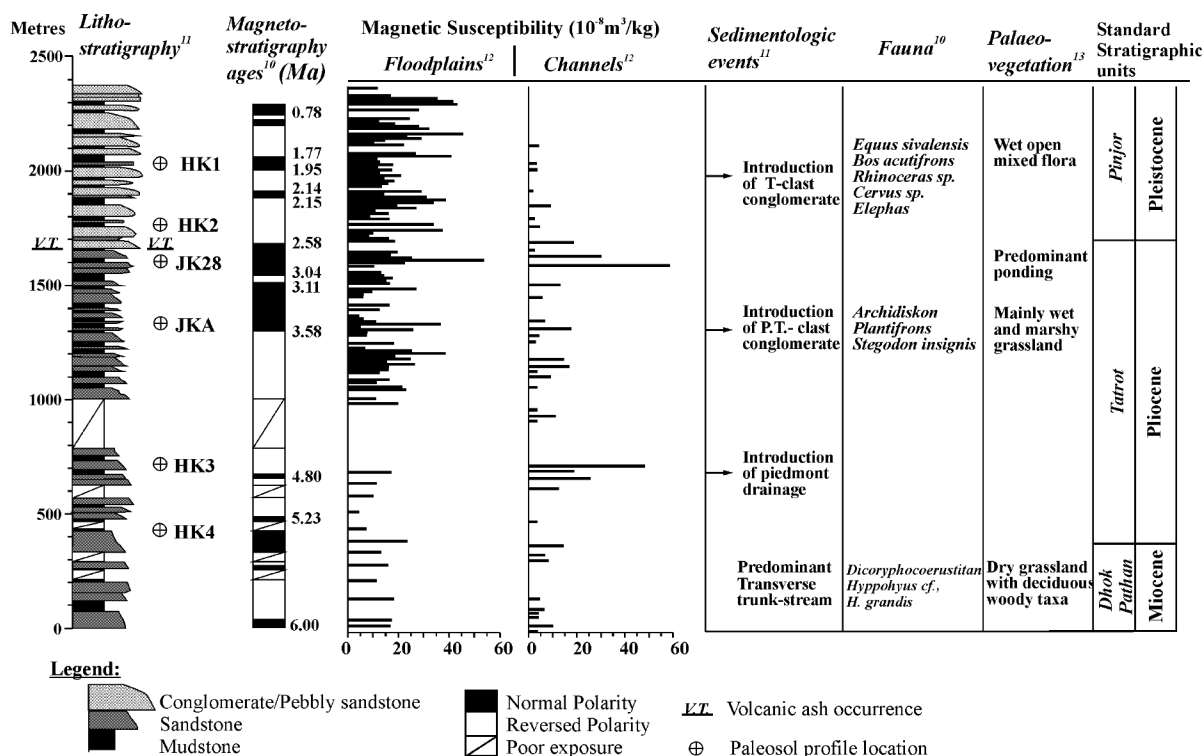


Figure 2. Correlation of lithology, magnetostratigraphy, magnetic susceptibility, sedimentologic events, faunal records and palaeo-vegetation information in the studied section near Hariipur, Nahan Dist. (HP).

measured using Molspin rock magnetometer. Since majority of the samples do not saturate till 4000 mT, a further IRM field at the intervals of 1000 mT was imparted to the maximum available field of 7000 mT, to confirm the occurrence of goethite.

An Anhysteretic Remanent Magnetization (ARM)² was induced by a constant biasing field of 0.1 mT simultaneously, with peak alternating field demagnetization of 100 mT at the decay rate of 0.01 mT per cycle, using DTECH demagnetizer with the ARM facility.

The studied magnetic and chemical parameters for the present investigation are described below.

The initial magnetic susceptibility (χ_{if}) is a bulk representation of ferromagnetic contents (plus paramagnetic components in weak samples). The χ_{if} -mean of 9×10^{-8} m³/kg for the 31 pedogenic levels of the studied section represents a relatively weak value comparable to antiferromagnetic assemblage (e.g. hematite: α -Fe₂O₃ and goethite: α -FeOOH)².

The frequency-dependence of magnetic susceptibility ($\chi_{fd}\%$) gives a broad estimate of grain-size of magnetic carriers. χ_{fd} is well below 6% for the studied samples (χ_{fd} -max = 6%), that indicates a Single Domain (SD) to Pseudo-Single Domain (PSD) range (0.03 μ m to ~ 20 μ m) of the magnetic minerals¹⁹.

The parameter of ARM susceptibility (χ_{ARM}) exclusively varies with the quantity of SD grains. In soil-forming conditions, the SD grains are typical of authi-

genic/biogenic magnetite that favours restricted/reducing environments²⁰.

IRM_{7T}, IRM_{(3-4)T}, IRM_{(1-0.5)T}, etc. are the stages of isothermal remanent magnetizations acquired when the fields referred in the subscript parenthesis are imparted (1T = 1000 mT). The acquired remanence is calculated by normalizing the weight of samples and expressed in the units of 10⁻⁵ Am²/kg.

SIRM represents the saturation of isothermal remanence (4T in present case), registering the contribution of ferrimagnetic and antiferromagnetic assemblage of minerals and the parameter is useful for relative quantification of both².

B_{0Cr} (remanence coercivity) is the field that reduces the SIRM to zero and is sensitive to magnetic mineralogy and grain size². The mean B_{0Cr} of 447 mT for the studied palaeosols indicates a very high coercivity, characteristic of the antiferromagnetic minerals (goethite and hematite)²¹.

IRM_{soft} is the parameter derived from 50 mT back-field IRM and approximates the remanence-carrying ferrimagnets.

Rb/Sr indicates the variation in chemical weathering or pedogenic intensity and is derived from the immobile versus mobile nature of these elements²².

TOC% and CaCO₃% are the approximation of total organic and inorganic carbon contents, respectively derived from the weight loss on combustion at 425 and 925°C in a muffle furnace.

A progressive rise in the partial SIRMs at 1, 2, 3 and 4 T (mean values of 82, 100, 106 and $117 \times 10^{-5} \text{ Am}^2/\text{kg}$, respectively) for the 31 studied pedogenic horizons infers the presence of high-coercivity anti-ferromagnetic minerals. The IRM acquisition and its backfield characteristics (B_{0Cr} and IRM_{soft}) infer a multi-mineral assemblage and a large gradient of pedogenic modification within a profile. Further, detailed thermo-magnetic characteristics and close-interval IRM spectra up to 7 T indicate the presence of goethite and hematite (details to be published elsewhere). Samples from majority of the profiles do not saturate even in this field and thus confirm the presence of goethite, which saturates at $\sim 20 \text{ T}^{(2)}$.

The ratio of goethite to hematite has been widely used by soil scientists to infer cold, humid and warm climatic phases, as a result of chemical processes controlled by soil Eh–pH, temperature and humidity (see Kampf and Schwertmann²³, Tardy and Roquin²⁴ and references therein). Moreover, Schwertmann²⁵ proposed 40°N latitude as a demarcation line in the northern hemisphere, to separate soils without hematite (northwards) from soils with hematite + goethite (south-

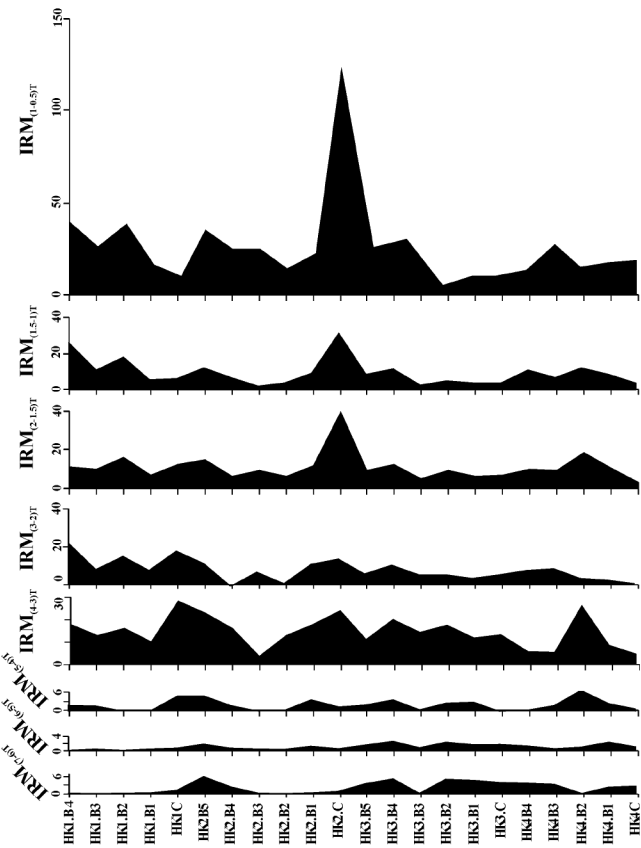


Figure 3. Contribution to IRM acquisition at different levels of applied field from 0.5 to 7 T. Note the maximum acquisition (magnitude) during $IRM_{(4-3)T}$ and $IRM_{(1-0.5)T}$ that has been related to goethite and hematite, respectively (see text for details). Units: Magnitude = $10^{-5} \text{ Am}^2/\text{kg}$ and Field = Tesla (1 T = 1000 mT).

Table 1. Hierarchical cluster analysis of the IRM contributions at different levels of acquisition remanence

Case	Two clusters	Three clusters	Four clusters	Five clusters	Six clusters
(I) $IRM_{(1-0.5)T}$	1	1	1	1	1
(II) $IRM_{(1.5-1)T}$	2	2	2	2	2
(III) $IRM_{(2-1.5)T}$	2	2	2	2	3
(IV) $IRM_{(3-2)T}$	2	2	2	3	4
(V) $IRM_{(4-3)T}$	2	2	3	4	5
(VI) $IRM_{(5-4)T}$	2	3	4	5	6
(VII) $IRM_{(6-5)T}$	2	3	4	5	6
(VIII) $IRM_{(7-6)T}$	2	3	4	5	6

wards). Hydroxylation due to hydrated–dehydrated cycles is quite common in the monsoon-fed tropical soils at seasonal scale and its intensity varies over millennial scale. Therefore, its influence can be recorded by deducing the relative abundance of goethite and hematite in the form of ratio of their quantitative magnetic saturation levels.

We plotted the IRM contributions at different levels of acquisition, from 0.5 to 7 T (Figure 3). The nature of peaks shows a notable change from high field (7 T) end towards the low field (0.5 T) end, depicting the maximum acquisition during $IRM_{(1-0.5)T}$ and $IRM_{(4-3)T}$ at the lower and higher ends, respectively. The level HK2C, conspicuously displays the maximum acquisition during $IRM_{(1-0.5)T}$, that decreases to $IRM_{(3-2)T}$ characterizing saturation IRM of hematite²¹. However, another peak originates at $IRM_{(4-3)T}$ level which vanishes by $IRM_{(7-6)T}$, suggesting association of hematite and goethite at HK2C. Another notable peak for the level HK4B2 at $IRM_{(4-3)T}$ behaves in a similar manner, characterizing the saturation for goethite²⁶ and relatively less hematite (see $IRM_{(1-0.5)T}$).

Table 1 shows the results of hierarchical cluster analysis of the data shown in Figure 3, obtained using ‘between-group-linkage’ method²⁷ for the eight cases of IRM acquisition plotted in the figure {e.g. Case (I): $IRM_{(1-0.5)T}$ denotes the IRM acquired by the samples between the applied field of 1000 mT and 500 mT}. The classification is made from two to six clusters, over the eight cases. It is notable that Cases (I) and (II) maintain a separate group (groups 1 and 2, respectively) throughout the classification from two clusters to six clusters, suggesting their acquisition characteristic of one mineral. Lowrie²⁸ inferred that hematite acquires about 80% of SIRM below 1 T of the applied field. Hence, Case (I), forming a separate group (= 1) throughout the classification in Table 1, is most characteristic of hematite. Similarly, Case (V) $IRM_{(4-3)T}$ appears to be the most representative range for goethite, supporting its maximum initial IRM acquisition characteristics^{21,26,29,30}. Moreover, with the higher order of classification, Case (V) forms a cluster nearest to Case (VIII) $IRM_{(7-6)T}$, that

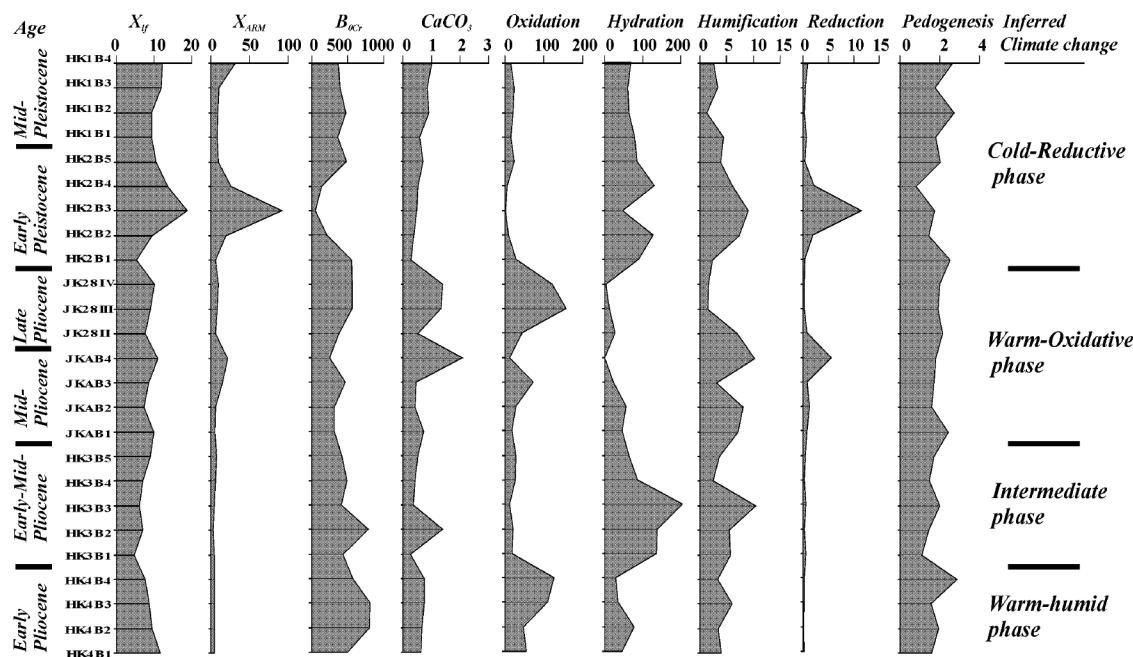


Figure 4. Magnetic and geochemical parameters for the studied pedogenic levels (exclusive of C-horizon) in the Haripur section in stratigraphic order. The new ratios introduced are: Oxidation = H/IRM_{soft} , Hydration = G/H , Humification = TOC/H , and Reduction = χ_{ARM}/H , where $G = IRM_{(4-3)T}$, $H = IRM_{(1-0.5)T}$. Pedogenesis (= Rb/Sr) is adapted from Chen *et al.*²² (see text for details).

again uniquely characterizes the high field saturation of goethite, supporting the above inferences. There are some peaks in disagreement with the above contention {e.g. HK3B5, HK3B4 and HK3B2 levels of $IRM_{(7-6)T}$; and HK4B2 levels of $IRM_{(2-1.5)T}$ }. Although it makes a small contribution ($< 5 \times 10^{-5} \text{ Am}^2/\text{kg}$), these disagreements are probably the result of (a) the isomorphically substituted varieties of goethite and hematite^{24,31} and/or (b) the grain size-dependent response to $IRM^{21,29,30}$. Such varieties and the grain size variations are quite common in tropical-sub-tropical climates²⁴. Furthermore, the large time span of 5 Ma of the present study makes it obvious to experience a substantial climatic and source-water-chemistry variation that may give rise to a variety of isomorphous substitutions and grain size variations for goethite and hematite. To explain the aforesaid anomalous IRM peaks at high field, a critical elemental and microscopic analysis on the magnetic separates is needed to distinguish the substitution and grain size. This is beyond the scope of the present attempt.

Briefly, we find that the maximum percentage of IRM has been acquired at the two levels, $IRM_{(1-0.5)T}$ and $IRM_{(4-3)T}$, that are characteristic of hematite and goethite respectively. Therefore, we define the indices $G = IRM_{(4-3)T}$ and $H = IRM_{(1-0.5)T}$ to represent the relative hydroxylation to dehydroxylation conditions, and hence the ratio G/H is denoted as the hydration index. The authigenic magnetite which forms in restricted, reducing conditions is saturated well below 100 mT and

displays coercivity less than 50 mT, characterizing a soft remanence. Thus the IRM_{soft} parameter has been deduced by subtraction of 50 mT backfield from the SIRM. Therefore, a ratio of H/IRM_{soft} is indicative of relative oxidative to reductive conditions and is thus designated here as 'oxidation index'. Since χ_{ARM} represents the authigenic magnetite that favours the reducing conditions in soil-forming environment²⁰, the ratio χ_{ARM}/H has been used here to infer the relative changes in reductive conditions. The low B_{0Cr} values ($< 50 \text{ mT}$) are indicative of low-coercivity minerals (e.g. magnetite-titanomagnetite and maghemite) and the higher values ($> 100 \text{ mT}$) are characteristic of high-coercivity minerals (goethite and hematite)²¹. Therefore, the B_{0Cr} curve in Figure 4 depicts the relative variation of these minerals. The organic matter in soils is preserved in humic conditions, hence a ratio TOC/H has been used to infer the relative humification (Figure 4).

The carbonates in the studied section occur in sheet-like (phreatic/groundwater-related) and nodular (pedogenic) forms. In the Pliocene profiles from HK4B1 to JKAB2, ' CaCO_3 ' shows a positive relation to G/H (hydration index) and TOC/H (humification index), suggesting warm humid conditions (Figure 4). During JKAB3, the peak in CaCO_3 corresponds to drop in hydration as well as oxidation index, but increased humification and reducing (or restricted) conditions. The JK28III level indicates a conspicuous peak in oxidation index, with higher Rb/Sr (pedogenesis) and CaCO_3 suggesting warmer conditions with greater pedogenic activ-

ity. The interval HK2B3 shows a remarkable peak in X_{lf} , suggesting restricted/reducing conditions and decrease in pedogenesis, indicative of cold conditions during Early Pleistocene.

Thus a large gradient of pedogenic changes has been noticed in the studied section, that appears to be useful for regional correlation and climatic aspects during Plio-Pleistocene. The new ratios (indices) of reduction, hydration, oxidation and humification based on selective rock magnetic and geochemical properties, need to be tested in deriving broad climatic inferences for basin-wide regional application. The present study of the Siwalik palaeosols suggests that pedogenic magnetic mineral transformation is governed by the production of canted antiferromagnetic minerals during Pliocene and ferrimagnetic minerals during Pleistocene.

1. Burbank, D. W., Beck, R. and Mulder, T., in *Tectonic Evolution of Asia* (eds Yin, A. and Harrison, T. M.), Cambridge University Press, 1996, pp. 149–188.
2. Thompson, R. and Oldfield, F., *Environmental Magnetism*, Allen and Unwin Publ. London, 1986, p. 220.
3. Opdyke, N. D. and Channel, J. E. T., *Int. Geophys. Ser.*, 1996, **64**, 250–276.
4. Johnson, G. D., *Geol. Rundt, Bd.*, 1979, **66**, 192–215.
5. Barry, J. C., Johnson, N. M., Raza, S. M. and Jacobs, L. L., *Geology*, 1985, **13**, 637–640.
6. Gaur, R. and Chopra, S. R. K., *Nature*, 1984, **308**, 353–355.
7. Behrensmeyer, A. K., Wills, B. J. and Quade, J., *Palaeogeogr. Palaeoclimatol. Palaeoecol.*, 1995, **115**, 37–60.
8. Retallack, G. J., *Mem. Geol. Soc. India*, 1990, **32**, 36–51.
9. Srivastava, J. P., Verma, S. N., Joshi, V. K., Verma, B. C. and Arora, R. K., *Geol. Surv. India, Spec. Publ.*, 1988, **11**, 233–241.
10. Nanda, A. C., Sati, D. C. and Mehra, G. S., *J. Himalayan Geol.*, 1991, **2/2**, 151–158.
11. Kumar, R., Ghosh, S. K. and Sangode, S. J., *Geol. Soc. Am. Bull., Spec. Pap.*, 1999, **328**, 239–255.
12. Sangode, S. J., Kumar, R. and Ghosh, S. K., *Mem. Geol. Soc. India*, 1999, **44**, 221–248.
13. Phadtare, N. R., Kumar, R. and Ghosh, S. K., *Spec. Publ. Himalayan Geol.*, 1994, **15**, 69–82.
14. Sangode, S. J., Kumar, R. and Ghosh, S. K., *J. Geol. Soc. India*, 1996, **47**, 683–704.
15. Johnson, G. D. et al., *Palaeogeogr. Palaeoclimatol. Palaeoecol.*, 1982, **37**, 63–93.
16. Ranga Rao, A., Agarwal, R. P., Sharma, U. N., Bhalla, M. S. and Nanda, A. C., *J. Geol. Soc. India*, 1998, **31**, 361–385.
17. Mehta, Y. P., Thakur, A. K., Nand Lal, Shukla, B. and Tandon, S. K., *Curr. Sci.*, 1993, **64**, 519–521.
18. Retallack, G. J., *Geol. Soc. Am., Spec. Pap.*, 1988, **216**, 1–20.
19. Dearing, J. A., Dann, R. J. L., Lees, J. A., Loveland, P. J., Maher, B. A. and O'Grady, K., *Geophys. J. Int.*, 1996, **124**, 228–224.
20. Maher, B. A. and Thompson, R., *Quat. Res.*, 1992, **37**, 155–170.
21. Dunlop, D. J. and Ozdemir, O., *Rock Magnetism: Fundamentals and Frontiers*, Cambridge University Press, 1997, p. 573.
22. Chen, J., An, Z. S. and Head, J., *Quat. Res.*, 1999, **51**, 215–219.
23. Kampf, N. and Schwertmann, U., *Geoderma*, 1983, **29**, 27–39.
24. Tardy, Y. and Roquin, C., in *Weathering, Soils and Palaeosols* (eds Martini, I. P. and Chestworth, W.), Developments in Earth Surface Processes–2, Elsevier, 1992, pp. 407–443.
25. Schwertmann, U., *Soil Sci. Soc. Am. J.*, 1988, **52**, 288–291.

26. Dekkers, M. J. and Rochette, P. R., *J. Geophys. Res.*, 1992, **97**, 17291–17307.
27. Davis, J. C., *Statistics and Data Analysis in Geology*, John Wiley and Sons, 1986, pp. 502–515.
28. Lowrie, W., *Geophys. Res. Lett.*, 1990, **17**, 159–162.
29. Dekkers, M. J., *Geophys. J.*, 1989a, **97**, 323–340.
30. Dekkers, M. J., *Geophys. J.*, 1989b, **97**, 341–355.
31. Wells, M. A., Fitzpatrick, R. W., Gikes, R. J. and Dobson, J., *Geophys. J. Int.*, 1999, **138**, 571–580.

ACKNOWLEDGEMENTS. We are grateful to the staff of the Environmental Magnetic Laboratory, University of Liverpool, UK for the assistance and advice. We are also grateful to the Director, Wadia Institute of Himalayan Geology, for his encouragement. The study was supported by the award of BOYSCAST fellowship (HRU/BYS/A-08/98) of the Department of Science and Technology, Government of India, to S.J.S.

Received 4 October 2000; revised accepted 27 April 2001

Land cover assessment in Jammu & Kashmir using phenology as discriminant – An approach of wide swath satellite (IRS–WiFS)

P. K. Joshi*, Sarnam Singh, Shefali Agarwal and P. S. Roy

Indian Institute of Remote Sensing, 4, Kalidas Road, Dehradun 248 001, India

Climatic and seasonal variations guide the change in the internal features of vegetation and thus the vegetation mapping. A correlation between the vegetation units and the normalized difference vegetation index (NDVI) is established and the spatial distribution of phenology and seasonal distribution is deduced for mapping. High amount of spectral variability contributed by phenological phases made us generate a large number of clusters to distinguish features. The study has significance in the light of national development needs *vis-à-vis* advancement expected in the future indigenous and international remote sensing missions. The study suggests that multi-date data consider the variability and enables us to delineate the land use and land cover pattern of Jammu & Kashmir. The regional phyto-phenological classified map provides details on vegetation stratum. They can be an excellent source of data for understanding the land dynamic processes and human interventions in the region. The map derived can delineate finer, the biogeographical zones.

INDIA encompasses a variety of climate, ranging from tropical, subtropical, temperate to alpine. There are

*For correspondence. (e-mail: pkjoshi27@hotmail.com)